ENERGY RAMPS FOR THE HIGH-ENERGY BOOSTER OF THE FCC-ee COLLIDER

L. Valle*[1], A. Chance[2], I. Karpov[1]
[1]CERN, Geneva, Switzerland
[2]Université Paris-Saclay - CEA, Gif-Sur-Yvette, France

Abstract

The FCC-ee full-size booster synchrotron prepares electron and positron bunch trains alternately for all foreseen beam energies from 45.6 GeV to 182.5 GeV and operation modes such as filling the collider from scratch or top-up. Polarized bunches could furthermore be supplied for the beam energy calibration. The first two operation modes require optimizing the energy ramps and RF voltage programs to achieve the small transverse beam sizes for injection in the collider while maintaining longitudinal beam stability. Specifically, the ramp for the ZZ operating point has an energy overshoot to boost the synchrotron radiation damping effect. Beam stability issues at low energy can be mitigated by damping wigglers at the cost of a higher energy spread at extraction. Further optimizations reduce the RF power requirements for all cycles.

INTRODUCTION

The booster accumulates, then accelerates alternatively electron and positron beams before injection into the Future Circular Collider (FCC-ee), for the four foreseen beam energies, 45.6 GeV (ZZ), 80 GeV (WW), 120 GeV (ZH) and 182.5 GeV ($t\bar{t}$), with 112 800 MHz superconducting cavities. An extra 336 cavities will be installed for the $t\bar{t}$ mode. There are two main operation modes of the booster [1]: filling the collider from scratch with shorter booster cycle and maximum bunch charge, and the top-up mode with adaptable bunch charges. The present contribution focuses on the filling mode which combines highest bunch charges and shorter cycles.

The energy and voltage ramps for acceleration are optimized to ensure the beam meets the extraction requirements while minimizing peak and average RF power and homogenize dynamic power losses between all booster cycles. Semi-analytical tools to compute the energy and voltage ramps of the high-energy booster were developed for that purpose [2]. Once the energy ramp and filling factor are defined, the voltage ramp is matched to the evolution of the longitudinal emittance and energy spread turn by turn. This contribution proposes energy ramps for all operation modes, shows the impact of injection errors on the longitudinal beam sizes at extraction and evaluates the dynamic power losses and RF power requirements of all booster cycles.

* lina.valle@cern.ch

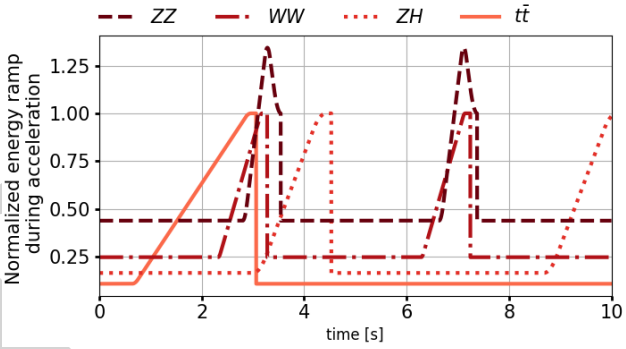

Figure 1: Energy ramps normalized to the extraction energy for all beam energies, displayed on a 10 s $t\bar{t}$ cycle.

ENERGY RAMPS FOR ALL BOOSTER CYCLES

Parabolic ramp round-offs are foreseen for the booster accelerating ramps for all operation modes. Figure 1 illustrates the foreseen energy ramps on the time scale of a $t\bar{t}$ 10 s booster cycle. The parabolae conserve the adiabaticity of the start and end of the accelerating ramp, by preserving the continuity of the energy gain. In all but ZZ mode, the energy gain is rapidly defined by the compensation of synchrotron radiation losses. The beam sizes then reach their natural values, defined by the equilibrium between radiation damping and quantum excitation [3, 4].

Turn by turn, the expected evolution of the longitudinal emittance following radiation damping and quantum excitation is calculated. The RF voltage is then matched to the longitudinal emittance. The voltage at flat top is adjusted to match the bunch length required for extraction. All voltage per cavity V_{cav} programs are displayed in Fig. 2. Further iterations will be needed depending on the location of the injection points of both the electron and the positron beams, which will change the desired energy of the injected bunches.

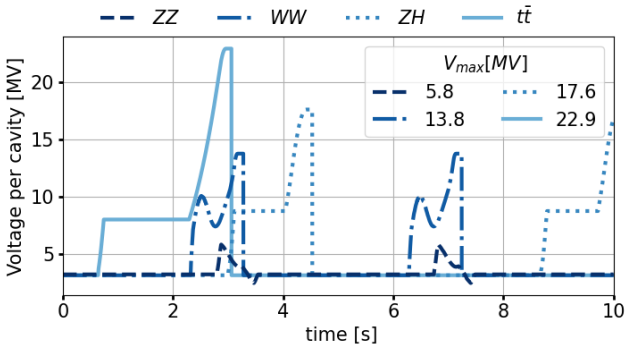

Figure 2: Example of the foreseen voltage per cavity V_{cav} programs for all beam energies, stacked on a 10 s $t\bar{t}$ booster cycle. ZZ mode includes an overshoot energy ramp [3, 4].

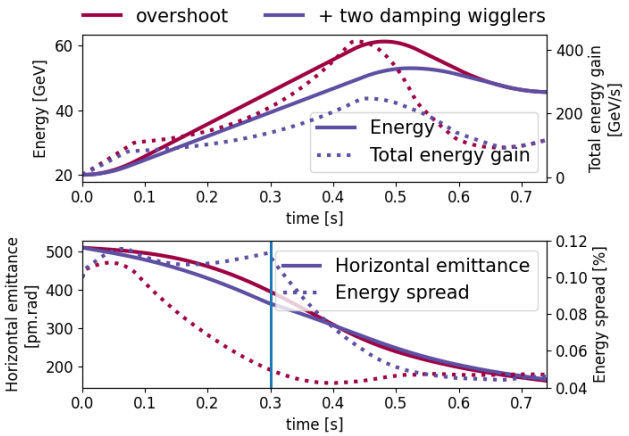

Figure 3: Comparison of two energy ramp strategies (top) for the ZZ mode, including an overshoot in energy and two damping wigglers. The later are disabled at an arbitrary time 0.3 s to allow natural damping of the beam energy spread. The bottom figure compares the evolution of the horizontal emittance (solid) and the energy spread (dotted) in both cases.

Overshoot Energy Ramp for the ZZ Mode

Injection simulations into the collider assume the electron and positron beams reach their natural beam sizes by the end of the booster ramp, with a maximum vertical emittance of 10 pm rad [5]. The transverse damping times at extraction energy, about 45.6 GeV, are equal to the duration of the accelerating ramp: the last bunches injected into the booster will therefore not experience enough radiation damping to reach the natural horizontal emittance $\epsilon_x = 87$ pm rad and natural energy spread $\sigma_E = 0.38 \times 10^{-3}$.

The booster cycle duration of the ZZ mode is fixed to comply with the collider intensity and maintain high luminosity [1]. Additionally, limits on the available accelerating gradient per cavity and the power converters of the booster magnets cap the accelerating gradient to 100 GeV/s. Therefore, a fast acceleration to 45.6 GeV to let the beam damp at flat top before extraction is not possible.

To boost damping and approach the extraction requirements, an overshoot to 60 GeV was needed for the energy ramp to reduce the horizontal emittance, as displayed in Fig. 3. The transition times between the different functions of the accelerating ramp and the target overshoot energy have been optimized using particle swarm optimization (PSO) [6]. Nonetheless, this approach alone is still not enough to reach the natural emittances for the ZZ mode.

Damping Wigglers for the ZZ Mode

The insertion of damping wigglers is foreseen to boost transverse radiation damping. Wigglers also open the possibility to use the booster as a photon source [7]. However, they blow the beam energy spread up. In a first approach, two damping wigglers (43 95 mm periods, 4.085 m effective length, 1 T peak magnetic field) were included at flat bottom and disabled mid-ramp to let the energy spread damp down to its natural value at 45.6 GeV. Figure 3 compares an overshoot ramp to 60 GeV without wigglers and an overshoot energy ramp to 55 GeV with damping wigglers disabled at $t = 0.3$ s in terms of energy lost per turn, horizontal emittance and energy spread at extraction. The option with damping wigglers requires less overshoot, less energy gain hence less voltage per cavity.

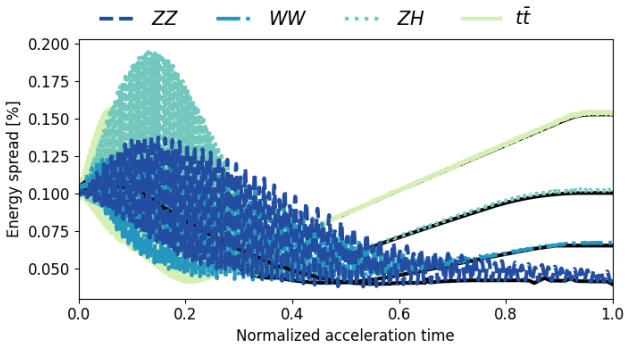

Figure 4: Impact of injection mismatches of 50 ps jitter and 0.3 % relative energy error on the energy spread at extraction of the last injected bunch for all foreseen energies. Solid black lines show the expected evolutions of the energy spread for all energies.

IMPACT OF INJECTION ERRORS ON THE LONGITUDINAL PARAMETERS AT EXTRACTION

Injection mismatches can be expected with maximum tolerances of 50 ps jitter and 0.3 % relative energy error. Impact of such errors on the beam sizes of the last injected bunches was simulated using the tracking code BLonD [8]. Figure 4 compares the evolution of the energy spread during acceleration for all foreseen energies, on a normalized timeline. For the highest energies, radiation damping suffices to damp the injection errors on the last injected bunch up to extraction. In the case of ZZ, the overshoot energy ramp without wigglers was used. The remaining longitudinal oscillations at extraction may be attenuated with the appropriate damping wigglers. Further optimization of the parameters of the damping wigglers is required both for beam sizes at extraction and mitigation of injection mismatches.

DISSIPATED POWER IN THE CAVITY WALLS

Dynamic power loss is the power dissipated in the RF cavity walls from their finite resistivity. The dynamic power loss is expressed as [9]:

$$P_{\mathrm{d}} = \frac{V_{\mathrm{cav}}^2}{2R_s} = \frac{V_{\mathrm{cav}}^2}{2(R/Q)Q_0} \tag{1}$$

with R_{s} the shunt impedance, Q_0 the unloaded quality factor, R/Q the normalized shunt impedance. Estimation of the dynamic power losses is essential for dimensioning the cryogenic system of the FCC-ee 400 MHz and 800 MHz cavities,

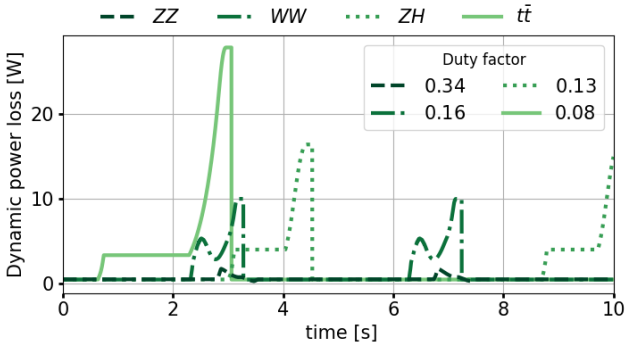

Figure 5: Evolution of the dissipated power in the superconducting 800 MHz cavity for all beam energies, following the voltage per cavity program in Fig. 2.

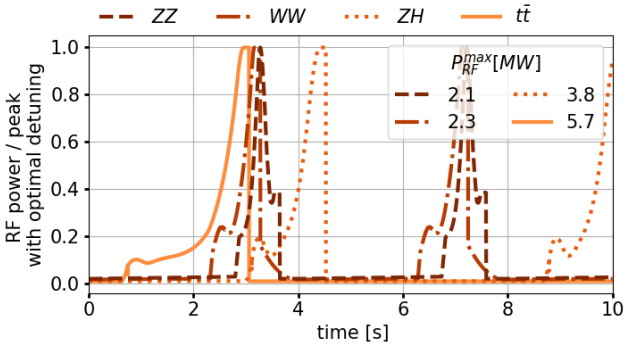

Figure 6: Normalized power requirements with regards to the peak power for all beam energies, displayed on the timescale of a 10 s tt̄ cycle.

Table 1: Dynamic power losses of the superconducting 800 MHz cavities in the booster.

Ramp mode	*ZZ*	*WW*	*ZH*	*tt̄*
Peak [W]	1.8	10	16	28
Average [W]	0.61	1.6	2.1	2.1
Integrated power [J]	2.4	6.5	12	21
Duty factor	0.34	0.16	0.13	0.08

and is displayed for the latter in Fig. 5. Table 1 lists the main figures of merit required for that purpose: the duty factor is the ratio between the average value of the dynamic power over its peak and the integrated power computes the total power to be handled by the cryogenic system during each booster cycle.

RF POWER AND TUNING REQUIREMENTS

Given a loaded quality factor Q_L and a detuning Δf, the required power to operate the cavity is expressed as [10]:

$$P_\mathrm{RF} = \frac{1}{2}(R/Q)Q_\mathrm{L} \times \left(\left[\frac{|V_\mathrm{cav}|}{2(R/Q)Q_L} + \frac{|F_\mathrm{b}|I_\mathrm{beam}\cos(\phi_\mathrm{f,d}+\phi_\mathrm{s})}{2}\right]^2 + \left[\frac{|V_\mathrm{cav}|}{R/Q} \times \frac{\Delta f}{f_\mathrm{RF}} + \frac{|F_\mathrm{b}|I_\mathrm{beam}\sin(\phi_\mathrm{f,d}+\phi_\mathrm{s})}{2}\right]^2\right) \quad (2)$$

with f_RF the RF frequency, $\phi_\mathrm{f,d}$ the focusing or defocusing cavity phase [11], F_b the form factor and I_beam the beam current. Since the booster RF system is shared between ZZ, WW and ZH, Q_L is fixed at 2.7×10^7. For tt̄, to ensure sufficient cavity bandwidth, the loaded quality factor is fixed at $Q_\mathrm{L} = 1\times10^7$ [1]. With a fixed voltage program and loaded quality factor, minimization of the power requirements can only be achieved with an optimal detuning program derived from Eq. (2):

$$\Delta f_\mathrm{opt} = -f_\mathrm{RF} \times \frac{|F_\mathrm{b}|(R/Q)I_\mathrm{beam}\sin(\phi_\mathrm{f,d}+\phi_\mathrm{s})}{2|V_{cav}|} \quad (3)$$

Comparison of the power requirements of all booster cycles including optimal detuning, is displayed in Fig. 6. RF power transients are discussed in Ref. [12]. As the cavity is powered, the radiation pressure from the electromagnetic wave deforms its walls, causing an additional Lorentz force detuning $\Delta f_\mathrm{L} = K_\mathrm{L} \times (V_\mathrm{cav}/L)^2$, with L the effective length of the cavity and K_L a material-dependent constant [9]. Its evaluation is essential for compensation strategies. Table 2 lists the values of peak power, average power and maximum tuning requirements for all booster cycles.

Table 2: Maximum power and tuning requirements for all booster cycles in the filling mode, considering both the optimal detuning Δf_{opt} and compensation of the Lorentz force detuning Δf_L, assuming $K_L = -1\,\mathrm{Hz}/(\mathrm{MV/m})^2$.

Mode	**ZZ**	**WW**	**ZH**	tt̄
P_{RF}^{max} [MW]	2.1	2.3	3.8	5.7
$< P_{RF} >$ [kW]	250	300	425	430
Δf_{opt}^{max} [Hz]	±1660	±500	±160	±35
Δf_L^{max} [Hz]	−27	−150	−250	−420

CONCLUSION

Semi-analytical tools were developed to optimize and adapt the FCC-ee booster energy ramps to all foreseen operation modes and beam energies. First proposals are double parabolic energy ramps and a voltage program matching the turn-by-turn evolution of the longitudinal emittance following radiation damping and quantum excitation. This principle minimizes quantities proportional to the voltage per cavity such as the RF power requirements and dynamic power losses. Additional features are needed for the ZZ mode to boost radiation damping and reach the requested extraction beam sizes. An overshoot energy ramp to 60 GeV respects the limit of 100 GeV/s on the accelerating gradient while reducing the horizontal emittance at extraction. Damping wigglers can be inserted in some booster straight sections. Further optimization is required to adapt the wiggler parameters to the needs of the high-energy booster. RF and cryogenics dimensioning strongly depend on the booster voltage per cavity program. The RF power requirements are minimized following an optimized detuning program for steady-state compensation of beam loading. The dissipated power in the cavity walls was evaluated and remains negligible compared to static heat loads.

REFERENCES

[1] M. Benedikt *et al.*, "Future Circular Collider Feasibility Study Report Volume 2", Rep. 19, 2025. doi:10.17181/CERN.EBAY.7W4X

[2] L. Valle, https://gitlab.cern.ch/lvalle/feb_fcc-ee.git

[3] A.Chance, "Overview of the booster status", presented at FCC week, Vienna, Austria, May 2025, https://indico.cern.ch/event/1408515/timetable/#49-overview-of-thebooster-sta,

[4] L. Valle, "Beam dynamics and rf requirements for the high-energy booster", presented at FCC week, Vienna, Austria, May 2025, https://indico.cern.ch/event/1408515/timetable/#98-beam-dynamics-and-rf-requir,

[5] G. Nigrelli, "First look at injection backgrounds", presented at FCC week, Vienna, Austria, May 2025, https://indico.cern.ch/event/1408515/timetable/#93-first-look-at-injection-bac,

[6] PYSWARMS, https://pyswarms.readthedocs.io/en/latest/index.html

[7] I. Agapov *et al.*, "Other Science Opportunities at the FCC-ee", CERN, Geneva, Rep., 2026. doi:10.17181/CERN.BSP4.H8ED

[8] H. Timko *et al.*, "Beam longitudinal dynamics simulation studies", *Phys. Rev. Accel. Beams*, vol. 26, no. 11, p. 114602, Nov. 2023. doi:10.1103/PhysRevAccelBeams.26.114602

[9] H. Padamsee, T. Hays, and J. Knobloch, *RF superconductivity for accelerators*. Weinheim, Germany: Wiley-VCH Verlag, Jan. 2008.

[10] J. Tückmantel, "Cavity-beam-transmitter interaction formula collection with derivation", CERN, Geneva, Switzerland, Tech. Rep. CERN-ATS-Note-2011-002-TECH, 2001. https://cds.cern.ch/record/1323893

[11] Y. Morita *et al.*, "Status of KEKB Superconducting Cavities and Study for Future SKEKB", in *Proc. SRF'09*, Berlin, Germany, Sep. 2009, paper TUPPO022, pp. 236–238. https://jacow.org/SRF2009/papers/TUPPO022.pdf

[12] L. Valle and I. Karpov, "RF power transients at injection energy in the FCC-ee high-energy booster", presented at IPAC'26, Deauville, France, May 2026, paper MOP7055, this conference.